KINETICS OF HEAT AND MASS TRANSFER BETWEEN A SPRAYED SOLUTION AND A HOT GAS FLOW

B. A. Belov, É. V. Gorozhankin,
and A. L. Suris

UDC 536.42:541.48

A two-zone mathematical model is given for the process of moisture evaporation from a sprayed solution and crystallization of the salt. The computer calculations are compared with the results of experimental work.

Plasma-chemical processes are widely used for the production of highly disperse materials from salt solutions [1]. Preliminary heat-treatment calculations make it possible to avert improper technological decisions and to adopt a well-substantiated approach to selecting the conditions for organization of the process, thereby reducing considerably the amount of exploratory or trial-and-error work. A dearth of experimental data and the enormous computational difficulties associated with modeling efforts make it impossible at the present time to devise a complete model of the processing of a solution in a plasma with allowance for the flow gasdynamics, the kinetics of phase transitions and chemical reactions, and the coalescence and comminution of particles. This situation has lent the greatest popularity to a one-dimensional model in which the material is assumed to fill the cross section of the duct uniformly [1-4]. This approach creates a considerable deviation of the results of calculations from the experimental data. The discrepancy is attributable to incomplete filling of the channel cross section with the jet of sprayed solution in the initial section, so that the temperature in the aerocolloidal zone is lowered appreciably and the evaporation length is increased.

In the present study we attempt to develop a two-zone model that takes into account the expansion of the jet zone along the length of the channel and the crystallization of the salt during moisture evaporation. Accordingly, we consider the flow in the reactor to consist of two zones with different temperatures. The sprayed solution moves in the gas flow in the inner (aerocolloidal) zone, and the hot heat-transfer agent moves in the outer zone. The boundary between the zones is formed by the trajectories of particles farthest from the channel axis. The properties of the gas flow in each zone within the cross section and normal to the axis of the channel are assumed to be constant. The mass flow rates of the gaseous phase at any time can be expressed by the equations

$$G_1 = (G_{T0} + G_V)(1 - f), \tag{1}$$

$$G_2 = (G_V + G_V) f. \tag{2}$$

The cross section of the jet can increase as a result of the radial dispersal of particles and also by the increase in the volume of the gaseous phase in the aerocolloidal zone with the evaporation of moisture, so that

$$\frac{df}{dx} = \frac{4\sqrt{f}\, w_R}{D_V w} + \frac{1 - f}{G_V + G_V} \frac{dG_V}{dx}. \tag{3}$$

Here the first term of the equation characterizes the dispersal of particles. The main force acting on the particles is aerodynamic drag, and so for the axial velocity of the particles we can write

$$\frac{dw}{dx} = C_D \frac{k_M}{k_v} \frac{\rho_2}{\rho} \frac{|w_2 - w|(w_2 - w)}{2wd}, \tag{4}$$

where C_D is the aerodynamic drag coefficient. The particle shape factors k_M (midsection of diametral) and k_V (volume) are given by the following identities for the area of the normal

---

Novomoskovsk Branch, State Scientific-Research and Design Institute of the Nitrogen Industry and Products of Organic Synthesis. Translated from Inzhenerno-Fizicheskii Zhurnal, Vol. 46, No. 5, pp. 797-804, May, 1984. Original article submitted November 26, 1982.

0022-0841/84/4605-0577$08.50

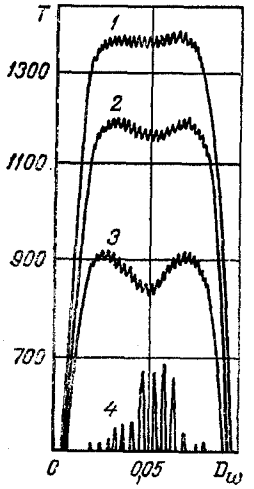

Fig. 1

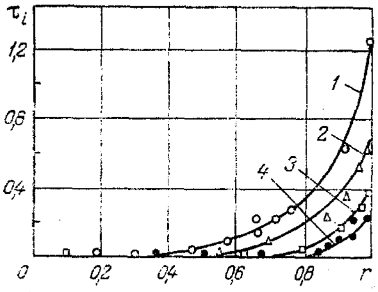

Fig. 2

Fig. 1. Radial temperature profile of the flow (T, K, vs D_w, m) for $x_V/D_w = 2$ and various relative mass flows of the sprayed solution. 1) $G_0/G_{T0} = 0.071$; 2) 0.2; 3) 0.35; 4) 0.48.

Fig. 2. Mean time τ_i, sec, between incidences of a single droplet on the thermocouple function vs volume fraction r of evaporated moisture, $d_3 = 1 \cdot 10^{-3}$ m. 1) $G_0 = 0.93 \cdot 10^{-3}$ kg/sec; 2) $2.4 \cdot 10^{-3}$; 3) $4.24 \cdot 10^{-3}$; 4) $6.48 \cdot 10^{-3}$.

(effective) cross section and volume of a droplet (respectively): $F_M = k_M d^2$ and $V = k_v d^3$. The droplet can be considered spherical within acceptable error limits for small Weber numbers, as are typical of small particles and small freestream velocities. For the radial dispersal velocity of the particles, which ultimately determines the diameter of the jet, we can write the following by analogy with (4):

$$\frac{dw_R}{dx} = -C_D \frac{k_M}{k_v} \frac{\rho_1}{\rho} \frac{w_R^2}{2wd}. \tag{5}$$

The aerodynamic drag coefficient depends on the shape of the particle and the flow regime around it and on the mass flow rate of vapor from the surface of the droplet. A great many relations have been proposed for the behavior of C_D as a function of the Reynolds number $\mathrm{Re} = |w_2 - w| d\rho_2 / 2\mu_2$, which is defined with respect to the freestream velocity. These functions yield close values for small numbers Re. However, the presence of a large vapor flow from the surface of the droplet, characterized by the Reynolds number $\mathrm{Re}_J = J_V d/2\mu_2$, tends to diminish C_D in comparison with the unevaporated droplet. It is advisable, therefore, to use the approximation given in [5], which takes this effect into account.

The flow temperature in the gaseous zone is lowered as a result of its cooling by the channel walls and can be described by the equation

$$\frac{dT_1}{dx} = -\frac{\pi \, \mathrm{Nu}_w \lambda_1 (T_1 - T_w)}{c_{p1} G_1}. \tag{6}$$

The Nusselt number for heat transfer to the channel walls for various flow regimes can be written in the form

$$\mathrm{Nu}_w = k_0 \left(\frac{w_1 \rho_1 D_w}{\mu_1}\right)^{k_1} \left(\frac{c_{p1}\mu_1}{\lambda_1}\right)^{k_2} \left(\frac{c_{p1}\mu_1}{\lambda_1}\right)_w^{k_3} \left(\frac{g D_w^3 \rho_1 \beta (T_1 - T_w)}{\mu_1^2}\right)^{k_4}, \tag{7}$$

where in the case of laminar flow [6] $k_0 = 0.15$, $k_1 = 0.33$, $k_2 = 0.68$, $k_3 = -0.25$, $k_4 = 0.1$, and for turbulent flow [7] $k_0 = 0.022$, $k_1 = 0.8$, $k_2 = 0.4$, $k_3 = k_4 = 0$.

The diameter of the drop decreases in moisture evaporation according to the equation

$$\frac{dd}{dx} = -\frac{2J_V}{\rho_{H_2O} w} \tag{8}$$

until the salt begins to crystallize. As in [8], we assume that the solid phase of the salt formed on the surface of the droplet "remembers" its size and thereafter remains unchanged until complete evaporation. Of course, thermoelastic stresses or the increased vapor pressure inside the solid salt sheath can cause it to burst and, after expulsion of the excess vapor, draw out once again into a film. Moreover, in the opinion of Styrikovich et al. [9], as much as 30%of the total mass of the solution is spattered away in the form of very minute droplets in the event of such bursts, creating further continuation of the sprayed material. The difficulties attending the description of this effect within the framework of the proposed model make it impossible to take coalescence and comminution into account, and so we write the balance of the total (net) flow of processed particles in the form

$$N_0 = \frac{G_0}{\rho_0 k_v d_0^3} = N = \frac{G}{\rho k_v d^3}. \tag{9}$$

The mass flow rate of vapor in the jet increases according to the equation

$$\frac{dG_V}{dx} = \frac{J_V F}{w}, \tag{10}$$

in which F = Nk$_F$d^2 is the surface area of all droplets in the flow. The temperature of the vapor—gas mixture in the jet zone is determined by the rate of admission of heat from the gaseous zone during expansion of the jet, by the heat transported with the disperse material, and by the superheat of the vapor:

$$\frac{dT_2}{dx} = \frac{1}{c_{p2} G_2} \left[\frac{4G_2 (H_1 - H_2) w_R}{\sqrt{f}\, D_w w} - (H_{V2} - H_V) \frac{dG_V}{dx} - \frac{\mathrm{Nu_T} \lambda_2 F (T_2 - T)}{dw} \right]. \tag{11}$$

The temperature of the particles increases to the boiling point of the solution and remains unchanged with the inception of crystallization. The spherical Hill vortex [10], which grows with flow around the droplet, has a characteristic relaxation time for its internal motion $\tau_\mu = \rho d^2/4\mu$, which is an order of magnitude smaller than the temperature equalization time inside the drop according to the molecular heat-conduction mechanism $\tau_\lambda = \rho d^2 c_p / 4\lambda$ and is three orders smaller than the equilization time of the salt concentration in the droplet due to molecular diffusion $\tau_D = d^2/4D_{H_2O}$. Consequently, the temperature and concentration profiles in the droplet can be regarded as gradient-free during the moisture evaporation time $\tau_e \gg \tau_D$. The heating of the particles is described by the equation

$$\frac{dT}{dx} = \frac{1}{c_p G w} \left[\frac{\mathrm{Nu_T} \lambda F (F_2 - T_1)}{d} - H_e J_V F + H_c \rho_c \lambda(c) F_c \right], \tag{12}$$

in which F$_c$ is the surface area of the crystals in the flow of sprayed material. Depending on the vapor pressure above the surface of the droplet, P$_d$, defined according to Thompson's law [11] as

$$P_d = P_V(c, T) \exp\left(\frac{4\sigma_p v_V}{RTd}\right), \tag{13}$$

moisture evaporation can take place in two regimes. If the pressure P$_d$ is lower than the pressure P$_w$ of the gas in the channel, the heat acquired by the droplet is dissipated in heating the material and in evaporating moisture. In the event of boiling of the solutions P$_d$ = P$_w$, and the heat acquired by the particle is spent in evaporation during exothermic crystallization or in evaporation and crystallization during endothermic crystallization. In the former case the evaporation process is limited by the diffusion of vapor from the surface of the drop into the flow, so that [1]

$$J_V = \frac{\mathrm{Nu}_D D_V \rho_V}{d} \ln\left(\frac{P_w - P_{V_2}}{P_w - P_d}\right). \tag{14}$$

The Nusselt numbers Nu$_T$ (thermal) and Nu$_D$ (diffusion) for the particle in the flow are determined according to approximate expressions [5], which take into account the shielding of the droplet surface by the vapor sheath.

Crystallization of the salt in the solution can take place through the primary nucleation of crystallization centers, which are stable for 10^{-12} to 10^{-10} sec and then either disintegrate or continue to grow, and also through the secondary nucleation and growth of existing crystals. According to the Gibbs–Volmer theory [12], for small supersaturations the typical length of the crystal nucleus can be specified as

$$l_{\mathrm{cr}} = \frac{2\sigma_{\mathrm{c}} M_{\mathrm{c}}}{3\rho_{\mathrm{c}} RT \ln (c/c_{\mathrm{s}})}, \tag{15}$$

and the rates of nucleation and growth of the crystals have the form

$$\alpha(c) = k_\alpha \exp\left[-\frac{k'_\alpha \sigma_{\mathrm{c}}^3 M_{\mathrm{c}}^2}{\rho_{\mathrm{c}}^2 R^3 T^3 \ln^2 (c/c_{\mathrm{s}})}\right], \tag{16}$$

$$\lambda(c) = k_\lambda \exp\left[-\frac{k'_\lambda \gamma_{\mathrm{c}}^2 M_{\mathrm{c}}}{\rho_{\mathrm{c}} R^2 T^2 \ln (c/c_{\mathrm{s}})}\right], \tag{17}$$

where k_α, k'_α, k_λ, and k'_λ are constants of the given salt. Disregarding secondary nucleation, the formal crystallization kinetics can be represented by the equations

$$\frac{dN_{\mathrm{c}}}{dx} = \frac{G - G_{\mathrm{c}}}{\rho w}\, \alpha(c), \tag{18}$$

$$\frac{dl_{\mathrm{c}}}{dx} = \frac{\lambda(c)}{w}. \tag{19}$$

For the precipitation of a salt consisting of n fractions with crystal lengths l_i and N_{ci} crystals in the fraction the mass flow rate of precipitate can be written as

$$G_{\mathrm{c}} = k_{\mathrm{vc}} \rho_{\mathrm{c}} \sum_{i=1}^{n} N_{\mathrm{c}i} l_i^3, \tag{20}$$

and the surface area of the crystals in the flow is

$$F_{\mathrm{c}} = k_{\mathrm{Fc}} \sum_{i=1}^{n} N_{\mathrm{c}i} l_i^2. \tag{21}$$

The concentration of salt in the solution can be determined from the expression

$$c = \frac{G_0 c_0 - \gamma G_{\mathrm{c}}}{G - G_{\mathrm{c}}}. \tag{22}$$

As moisture evaporates from the solution, the salt concentration increases and at some time we obtain a supersaturated solution with a typical length of the nucleus $l_{1\mathrm{cr}}$. Solving the system of differential equations (3)-(6), (8), (10)-(12), (18), (19), in the next integration step Δx we determine the number $N_{\mathrm{c}1} = N_{\mathrm{c}}$ and the size $l_1 = l_{1\mathrm{cr}} + l_{\mathrm{c}}$ of the crystals in the first fraction, along with the critical size $l_{2\mathrm{cr}}$ of the nucleus in the second step. Then in any j-th integration step we determine the linear dimensions and number of crystals in the precipitate flow:

$$l_i = l_{i\mathrm{cr}} + \Delta l_{\mathrm{c}}\big|_{x=x_{i-1}}^{x=x_j}, \quad N_{\mathrm{c}i} = \mathrm{const} \quad (i < j),$$

$$l_i = l_{i\mathrm{cr}} + \Delta l_{\mathrm{c}}\big|_{x=x_{j-1}}^{x=x_j}, \quad N_{\mathrm{c}i} = \Delta N_{\mathrm{c}}\big|_{x=x_{j-1}}^{x=x_j} \quad (i = j).$$

The given system of equations for the heat- and mass-transfer kinetics of the sprayed solution has been solved numerically by the familiar Runge–Kutta method in Merson's modification for a sodium chloride solution in an air flow. The thermophysical properties of the substances were taken from [13], and the kinetic crystallization constants were obtained by processing the results of [14].

To compare the results of the calculations with experiment we have investigated the process of moisture evaporation in a channel with an inside diameter $D_{\mathrm{w}} = 0.1$ m for flows with a mass injection rate $G_0/G_{T0} = 0.06$-0.48 and a heat-transfer agent at an initial temperature $T_{T0} = 3200$-3600°K. The sodium chloride solution was injected into a conical three-

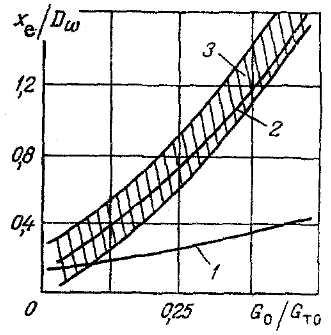

Fig. 3

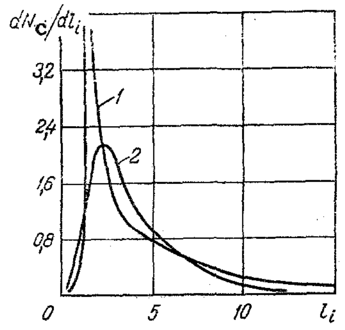

Fig. 4

Fig. 3. Moisture evaporation length vs. content of sprayed solution in the flow. 1) Calculated according to single-zone model; 2) calculated according to two-zone model; 3) spread of experimental data.

Fig. 4. Differential frequency—size distribution function of NaCl crystals, $D_w/d_0 = 670$, $G_0/G_{T0} = 0.25$, $T_{T0} = 3500°K$ (l_i, μm). 1) Experimental; 2) calculated.

jet mixing chamber along the duct axis of a pneumatic atomizer. The initial droplet size distribution, which was determined in special tests by a collecting procedure in an immersion medium, is described within 10% error limits by the Rosin—Rammler distribution [15]

$$\frac{\sum_{j=i}^{n} N_j d_{j0}^3}{\sum_{j=1}^{n} N_j d_{j0}^3} = \exp\left[-\left(\frac{d_{i0}}{1{,}4\cdot 10^{-4}}\right)^{2,2}\right]. \tag{23}$$

Droplets with diameters ranging from 2 to 300 μm were observed in the actual spraying operation. The mean diameters, defined as

$$d_{mk} = \left(\sum_{i=1}^{n} d_i^m N_i \Big/ \sum_{i=1}^{n} d_i^k N_i\right)^{\frac{1}{m-k}},$$

where m and k are integers, were equal to $d_{32} = 100\text{-}200$ μm, depending on the operating conditions of the atomizer, with a homogeneity criterion $h = (d_{32}/d_{20})^2$ [16] equal to 4.5-7.

The radial temperature profile was determined by means of a slowly moving thermocouple at various duct lengths. The temperature so obtained differs in every case from the temperature of the gas flow, because the thermocouple junction loses heat through radiation onto the duct wall. It is difficult to determine the wall temperature in working with salt solutions, because the crust deposit on the walls has different thicknesses, and so its temperature varies along the duct and with time. Typical experimental results are shown in Fig. 1. It is seen that a temperature reduction in the axial region occurs even at relatively great lengths. Complete moisture evaporation is not observed for a large content of disperse material in the flow, a fact that is manifested in random temperature fluctuations of the junction when a liquid droplet is incident on it. It is important to note the "pulsating behavior" of the recorded temperature, as it evinces fluctuations of the heat flux onto the function.

The probability of a single droplet of diameter d_j hitting a spherical junction of diameter d_3 is equal to $(d_j + d_3)^2/D^2$. During the probing period τ_i the number of particles of diameter d_j traversing the cross section of the duct in which the thermocouple is moving is equal to $\tau_i N_j$, so that the probability of at least one droplet of diameter larger than d_i hitting the junction in the case of a polydisperse flow is equal to

$$W_i = \frac{\tau_i}{D^2} \sum_{j=i}^{n} N_j (d_j + d_3)^2. \tag{24}$$

Setting the right-hand side of expression (24) equal to unity, we find the mean time τ_i during which an unevaporated particle is recorded. It is evident from Fig. 2 that τ_i increases with a decrease in the mass flow of raw material. For a specified probability p of a droplet being detected by the junction the required probing period is $\tau=-\tau_i\ln(1-p)$. The mean time τ_i is chosen to minimize the mass flow of raw material. For polydisperse spraying we take the length over which at least 95% of the moisture is evaporated as the evaporation length.

The evaporation lengths determined experimentally and calculated according to the single-zone and two-zone models are shown in Fig. 3. The results of both models are close for small mass flows of disperse material, owing to the small reduction in the temperature of the gas flow in the jet. When G_0/G_{T0} is increased to 0.48, the discrepancy between the single-zone model and experiment attains 400%, whereas the two-zone model describes the experimental data satisfactorily. The large scatter of x_e/D_w obtained in the model setup is associated with the polydispersity of the real spray.

The size distribution of NaCl crystals is shown in Fig. 4. The experimental curve has been obtained by counting the number and calculating the sizes of the salt crystals visible on electron micrographs. The median dimension (side) of the fact of near-cubic crystals is d_{10} = 1.9 μm, and the homogeneity criterion h = 3.5. If we assume that only one salt crystal is obtained from one droplet of solution, the median diameter must be 10-20 μm, which is an order of magnitude greater. This indicates that crystallization takes place in the droplet through the formation of several small crystalline particles. A certain shift between the maxima of the theoretical and experimental distribution functions can be attributed to insufficient accuracy of the kinetic parameters of the salt crystallization process. Any influence of the mass flow of solution and of the operating conditions on the shape of the distribution curve was not detectable.

NOTATION

$\alpha(c)$, nucleation rate; β, coefficient of cubical expansion; c, concentration; c_p, specific heat; D, diameter, diffusion coefficient; d, typical particle size; F, surface area; f, degree of filling of the duct by the jet; G, mass flow rate; γ, mass fraction of anhydrous salt in crystalline hydrate; J, mass flow rate of vapor from particle surface; l, typical length of crystals; λ, thermal conductivity; $\lambda(c)$, linear growth rate of crystals; M, molecular weight; μ, viscosity; k, a coefficient; N, particle flux; n, number of fractions; P, pressure; R, universal gas constant; ρ, density; σ surface tension; τ, time; v, molar volume; w, axial velocity; w_R jet expansion rate; $\varkappa$, linear tension; H, heat (quantity); x, duct length. Indices: 0, initial state; 1, gaseous zone; 2, aerocolloidal zone; d, droplet surface; e, evaporation; i, i-th component; c, crystals; cr, critical state; M, midsection; s, saturated; V, vapor; S, solution; H_2O, water; v, volume; F, surface (area); w, duct wall; T, heat-transfer medium.

LITERATURE CITED

1. Yu. N. Tumanov, Electrothermal Reactions in Present-Day Chemical Technology and Metallurgy [in Russian], Énergoizdat, Moscow (1981).
2. S. A. Panfilov, Yu. V. Tsvetkov, I. K. Tagirov, and D. M. Chizhikov, "Application of mathematical modeling to assess the behavior of powdered elements and compounds introduced into a low-temperature plasma jet," in: Low-Temperature Plasma Generators [in Russian], Énergiya, Moscow (1969), pp. 48-59.
3. I. L. Mostinskii and D. I. Lamden, "Heat and mass transfer in the phase transitions of solutions dispersed in a high-temperature gas flow," in: Proc. Fifth All-Union Conf. Heat and Mass Transfer [in Russian], Vol. 3, ITMO Akad. Nauk BSSR, Minsk (1976), pp. 190-194.
4. I. S. Burov and A. L. Mossé, "Numerical calculation of the heating of silicon dioxide in a multijet plasma reactor," in: Abstr. Third All-Union Symp. Plasma Chemistry [in Russian], Vol. 2, Nauka, Moscow (1979), pp. 79-82.
5. A. M. Golovin and V. R. Pesochin, "Evaporation of a droplet of a solution in a high-temperature medium," Teplofiz. Vys. Temp., 14, No. 4, 814-822 (1976).
6. Chemistry Handbook [in Russian], Vol. 5, Khimiya, Moscow–Leningrad (1966).
7. V. I. Rozhdestvenskii, "Experimental study of heat transfer associated with turbulent air flow in a circular tube with large differential temperatures in the cooling case," Zh. Prikl. Mekh. Tekh. Fiz., No. 3, 112-115 (1979).

8. M. V. Lykov and B. I. Leonchik, Spray Dryer [in Russian], Mashinostroenie, Moscow (1966).
9. M. A. Styrikovich, Yu. A. Zakhorko, I. L. Mostinskii, et al., "Problems of injecting and extracting the ionizing additive in the U-25 apparatus," Teplofiz. Vys. Temp., 2, No. 2, 440-445 (1974).
10. H. L. Lamb, Hydrodynamics, Macmillan, London (1932).
11. Course in Physical Chemistry [in Russian], Vol. 1 (edited by Corresponding Member of the Academy of Sciences of the USSR Ya. I. Gerasimov), Khimiya, Moscow (1973).
12. E. V. Khamskii, Crystallization from Solutions [in Russian], Nauka, Leningrad (1967).
13. N. B. Vargaftik, Handbook of Thermophysical Properties of Gases and Liquids [in Russian], Nauka, Moscow (1972).
14. F. Rumford, "The controlled crystallization of sodium chloride," Ind. Chem. Eng., 38, No. 1, 10-20 (1960).
15. D. G. Pazhi and V. S. Galustov, Liquid Atomizers [in Russian], Khimiya, Moscow (1979).
16. Vile Madr, Sbornik vědeckých Praci Vydoré skoly baňskě Ostravě Ročnik XVIII, čislo 2, řada hornickogeologicka, clanek 319 (1972), p, 133.

COMPENSATING PARASITIC HALL CURRENTS IN A MHD GENERATOR HAVING TEMPERATURE INHOMOGENEITY IN THE PLASMA FLOW

A. A. Beloglazov and B. M. Berkovskii

UDC 621.313.12:538.4

The inhomogeneity parameter is examined as a function of the variation in current density over the cross section. It is pointed out that this parameter can be determined without measuring the conductivity in the cross section.

In several papers [1-8] it has been pointed out that MHD characteristics can be improved by changing the current density in the cross section of the channel by tapping off current in the magnetic-field direction. Here we introduce the inhomogeneity parameter, which incorporates not only the plasma inhomogeneity but also the inhomogeneity in the current density in the cross section, and it is used to examine the improvement in MHD characteristics. We write the expression for the Hall current by using the projections of Ohm's law on the coordinate axes and averaging them in the direction of the Y and Z axes:

$$E_x = \frac{\left(\left\langle\!\left\langle \frac{j_x}{j_y} \right\rangle\!\right\rangle + \langle\!\langle \beta \rangle\!\rangle\right)\left(\langle\!\langle E_y \rangle\!\rangle - \langle\!\langle U \rangle\!\rangle B + \frac{\langle\!\langle \beta \rangle\!\rangle \left\langle\!\left\langle \frac{j_x}{j_y} \right\rangle\!\right\rangle}{\langle\!\langle \sigma/j_y \rangle\!\rangle}\right)}{\langle\!\langle \sigma/j_y \rangle\!\rangle \left\langle\!\left\langle \frac{(1+\beta^2)\, j_y}{\sigma} \right\rangle\!\right\rangle - \langle\!\langle \beta \rangle\!\rangle^2}. \tag{1}$$

The denominator in (1) is

$$G_B = \langle\!\langle \sigma/j_y \rangle\!\rangle \left\langle\!\left\langle \frac{(1+\beta^2)\, j_y}{\sigma} \right\rangle\!\right\rangle - \langle\!\langle \beta \rangle\!\rangle^2 \tag{2}$$

and by analogy with [6, 9, 10] it is called the inhomogeneity parameter. Also, (2) contains j_y explicitly, which enables one to choose the j_y profile to minimize the inhomogeneity parameter and thus improve the MHD generator characteristics. One can influence the distribution of j_y in the cross section for example by profiling the section, and also by profiled injection, the choice of loading system, profiling the temperatures of the current-collecting surfaces, and profiling the conductivities of the electrode materials.

We use a stationary two-dimensional electrodynamic formulation to demonstrate the effects of current-density variation over the cross section on the inhomogeneity parameter.

High-Temperatures Institute, Academy of Sciences of the USSR, Moscow. Translated from Inzhenerno-Fizicheskii Zhurnal, Vol. 46, No. 5, pp. 804-808, May, 1984. Original article submitted December 20, 1982.

0022-0841/84/4605-0583$08.50